

¹ Department of Photogrammetry and Geoinformatics, Lviv Polytechnic National University, 12, S. Bandera str., Lviv, Ukraine, 79013, tel. +38(096)4143409, e-mail: ivanchuk_oleh@ukr.net

² Department of Photogrammetry and Geoinformatics, Lviv Polytechnic National University, 12, S. Bandera str., Lviv, Ukraine, 79013, tel. +38(050)7455711, e-mail: ol.tums@gmail.com

A STUDY OF FRACTAL AND METRIC PROPERTIES OF IMAGES BASED ON MEASUREMENTS DATA OF MULTISCALE DIGITAL SEM IMAGES OF A TEST OBJECT OBTAINED

<https://doi.org/10.23939/istcgcap2017.01.053>

Purpose. The goal of this work is to establish and study the fractal and metric characteristics of images obtained with scanning electron microscopes (SEM). **Methods.** This approach is based on the processing of measurements data of digital SEM images of a test object obtained on four types of modern SEM in the magnification range from 1000^x to 30000^x . **Results.** The analytical relationship between the increase that was set on the device scale and the “fractal” increase (scale) is established. The similar coefficients A_{xf} (A_{yf}) and the exponential factors D_{xf} (D_{yf}) for fractal magnifications (scales) along the x and y axes are calculated for 4 types of SEM. Formulas are obtained for calculating the possible range magnifications of the images of test object depending the test object spacing, pixel size and scale. The obtained relationships for the calculation of fractal scales allow to automatically determine the real increase (scale) of SEM images and using the calculated coefficients of the polynomials, effectively eliminate their distortions. **Scientific novelty.** The technique developed by the authors for obtaining fractal and metric characteristics of SEM images was performed for the first time in Ukraine. The proposed methodology is accompanied at all stages by the author's software and demonstrated its effectiveness and expediency. **The practical significance.** The application of this method of establishing and accounting for the fractal and metric characteristics of digital SEM images makes it possible to more precisely determine the real values of the increases (scales) of digital SEM images and the values of their geometric distortions. Taking into account these characteristics of SEM images makes it possible to significantly improve the accuracy of obtaining spatial quantitative parameters of the micro surfaces of research facilities, and consequently improve their operational and economic characteristics. The obtained characteristics can be additional important quantitative parameters for revealing the features of digital SEM images.

Key words: scanning electron microscope (SEM); the test object; digital SEM image; fractal and metric properties of digital SEM images; real increase (scale), geometric distortion of digital SEM images.

Introduction

Calibration of digital SEM images, that is, the determination of their true scales and geometric distortions, is an important technological link in the photogrammetric processing of SEM stereopairs of research objects for the calculation of their spatial quantitative characteristics with the required accuracy. Much attention was paid to the problems of determining the real scales of SEM images, their geometric distortions, and their accounting from the time of creation from the first SEM to the advent of SEM with digital image recording. To date, these problems are almost solved. They are based on the SEM calibration method using photogrammetric image processing of SEM of special test objects with standard resolution characteristics (test grids, holographic gratings, etc.). The most important publications on this subject are given in the bibliography [Ivanchuk, Khrupin, 2012; Ivanchuk,

2012, 2013, 2014, 2015; Ivanchuk, Barfels, Heeg, Heger, 2013; Ivanchuk, Chekajlo, 2014; Ivanchuk O., Tumska, 2016, 2017; Kostyshyn, Mustafin, 1982; Kalantarov, Sagyndykova, 1983; Melnik, Sokolov, Ivanchuk, Tumska, Shebatinov, 1984; Bovik, 2000; Boyde, 1975; Burkhard, 1980; Ghosh, 1975, 1976; Howell, 1975].

However, just a few works have been devoted to the study of SEM images of multi scales from the point of view of their possible fractal nature, as well as to the obtaining of various numerical characteristics that confirm or disprove the view that SEM images also have *scaling* properties, that is, scale invariance or self-similarity.

Analysis of the latest research and publications devoted to solving this problem

The principles of fractal geometry in the practice of SEM-stereophotogrammetry were first

applied to studies of microstructure of soils by V. M. Melnik and V. M. Sokolov [Melnik, Sokolov, 1993; Melnik., Voloshin, Tarasyuk, Blinder, 1999]. The principles of fractality were also used in studies of the mechanics of metal destruction by SEM images of their micro surfaces [Melnik, Bobro, Shostak, Voloshin, 1996; Bobro, Melnik, Voloshin, Shostak, 1997]. The method of fractal analysis was applied by V. M. Melnik and V. U. Voloshin to assess the destructive changes in bone tissue of animals due to their radiation exposure [Melnik, Voloshin, 2002]. Theoretical and practical results of using the principles and theoretical assumptions of fractal geometry in the processing of SEM images of various micro surfaces are generalized and described in the monograph by V. M. Melnik and A. V. Shostak [Melnik, Shostak, 2009; Shostak, 2012].

However, the authors did not find works in which such approaches would be used to study the metric characteristics of SEM images.

Description of the approach and research results

The stochastic nature of the process of obtaining SEM images (the current of secondary electrons), as well as random quantities of the intensity (the gray level) can be considered the cause of the fractal nature of SEM images.

We have noticed that for different magnifications, SEM images have a *scaling* property, that is, scale invariance or self-similarity. Since the real increases (scales) of the SEM image along the x and y axes as a result of various distortions in the process of its formation, as a rule, somewhat differ from each other. We can consider them self-affine, not self-similar [Feder, 2012].

Multiscale SEM images can be attributed to the type of statistically similar fractal sets based on the definition of metric dimension, strictly greater than the topological dimension [Anishchenko, Vadivasova, 2010]. An example of natural fractals of this type is a fragment of the coastline [Richardson, 1961].

As shown in the works of Ivanchuk O. M. [Ivanchuk, 2012, 2013, 2014, 2015; Ivanchuk, Barfels, Heeg, Heger, 2013; Ivanchuk, Chekajlo, 2014], the values of real scales of SEM images are non-integer and differ from those established on the

device scale. The increases in the SEM image of M_x and M_y are determined from 8 measured centers of the test object (test grid) nodes in the central part of the image (see the photos in Table 3). The distance values are calculated from the coordinates of the node centers in the magnification scale. Real scales are defined as the average value of the ratio of the distances between the centers of nodes in the scale of magnification to the corresponding distances between the nodes of the test grid.

As a result the experimental values of the series of real scales for various SEMs for fixed magnification values the following sets on the device scale were obtained [Ivanchuk, 2012, 2013, 2014; Ivanchuk, Barfels, Heeg, Heger, 2013]:

– 1000^x, 2000^x, 5000^x, 8000^x, 10000^x, 15000^x, 20000^x, 24000^x, 27000^x, 30000^x for SEM JCM-5000 (NeoScope) (JEOL, Japan);

– 2000^x, 5000^x, 7500^x, 10000^x, 15000^x, 20000^x, 25000^x, 30000^x for SEM JSM 7100F (JEOL, Japan);

– 1000^x, 2000^x, 3000^x, 5000^x, 10000^x, 20000^x for SEM DSM-960A (Zeiss, Germany);

– 1000^x, 2500^x, 5000^x, 8000^x, 10000^x, 15000^x, 20000^x, 25000^x for SEM 106I (Sumy, Ukraine).

The main technical specifications of SEM, used in obtaining digital SEM images of the test grid are given in Table 1.

Analysis of the obtained results shows that when the scale is changed then the distance between nodes of the test grids do not change strictly in proportion to the scale ratio the set on the device scale, but they increase in a non-integer number of times.

Based on the empirical relationship obtained by Richardson [Richardson, 1961], the authors established a scale ratio between the fixed (integer) increase M set on the scale of the device in SEM and the “fractal” increase value M_f [Ivanchuk, Tumska, 2016]:

$$M_f = A_f \cdot M^{2-D_f}, \quad (1)$$

where A_f is the proportionality coefficient; D_f is an exponential factor. The scale M_f calculated by (1) will be called the *fractal* scale. If we denote the true test grid spacing by r , then, with an increase of M times, the real length of the spacing, according to (1) is

$$M_f \cdot r = A_f \cdot (M \cdot r) \cdot M^{1-D}. \quad (2)$$

In [Mandelbrot, 1983] it was shown that the value of D_f is a fractal dimension.

The values of A_f and D_f are determined from the set of pairs of values of integer and real scales (M, M_{xr}) , (M, M_{yr}) along the x and y axes, respectively. For the different types of SEM, the graphs of the logarithms of real scales M_{xr} (M_{yr}) against the logarithms of integer scales M represent straight lines (see Fig. 1).

It should be noted that the graphs for JCM-5000 and JSM 7100F almost coincide. While for DSM-960A and SEM 106I, the graphs are shifted along the logarithmic y axes by 0.3 and 0.45 respectively, and differ from the increases that set on the device scale by approximately 2 and 3 times. The

parameters of the lines (Fig. 1) are determined from the regression equations.

Determination of the parameters of the regression equation. Substituting into the equation (1) instead of M_f , the known values of M_r after logarithm, we are

$$\lg M_r = \lg A_f + (2 - D_f) \cdot \lg M \quad (3)$$

If we denote

$$x = \lg M, \quad y = -\lg M_r, \quad A = 2 - D_f, \quad C = \lg A_f, \quad (4)$$

then we obtain the equation of a straight line and find it's parameters that [Cromley, 1992]:

$$\min \sum_{i=1}^N (s_i)^2, \quad (5)$$

Table 1

The main technical specifications of SEM and digital SEM images

| SEM | JCM-5000 (NeoScope) | JSM 7100F | DSM-960A | SEM 106 I |
|--------------------------------|------------------------------------|------------------------------------|------------------------------------|------------------------------------|
| Observation mode | high-vacuum | high-vacuum | high-vacuum | high-vacuum |
| Accelerating voltage | from 5 to 15 kV | from 0.5 to 40 kV | from 1 to 30 kV | from 0.5 to 30 kV |
| Magnification range | from 10^x to 40000^x | from 10^x to 300000^x | from 10^x to 100000^x | from 15^x to 300000^x |
| Maximum specimen size, mm | diameter up to 70, height up to 50 | diameter up to 70, height up to 50 | diameter up to 70, height up to 50 | diameter up to 50, height up to 30 |
| Spatial resolution | 10 nm | 1.2 nm | 5 nm | 2 nm |
| Digital image, pixels | 1280×1080 | 1280×1024 | 800×600 | 1280×960 |
| Pixel size, mm | 0.09132 | 0.09375 | 0.13698 | 0.09375 |
| Pixel size, mm | 0.09132 | 0.09375 | 0.26450 | 0.26450 |
| Coeff. of transition to M real | 1.0 | 1.0 | 1.9310 | 2.8213 |
| Image size, mm | 116.9×98.6 | 120.0×96.0 | 211.6×158.7 | 338.6×253.9 |
| Image file format | JPEG, TIFF | BMP, JPEG, TIFF | JPEG, TIFF | BMP |
| Image file size, Mb | 1.32 | 1.25 | 0.47 | 1.17 |

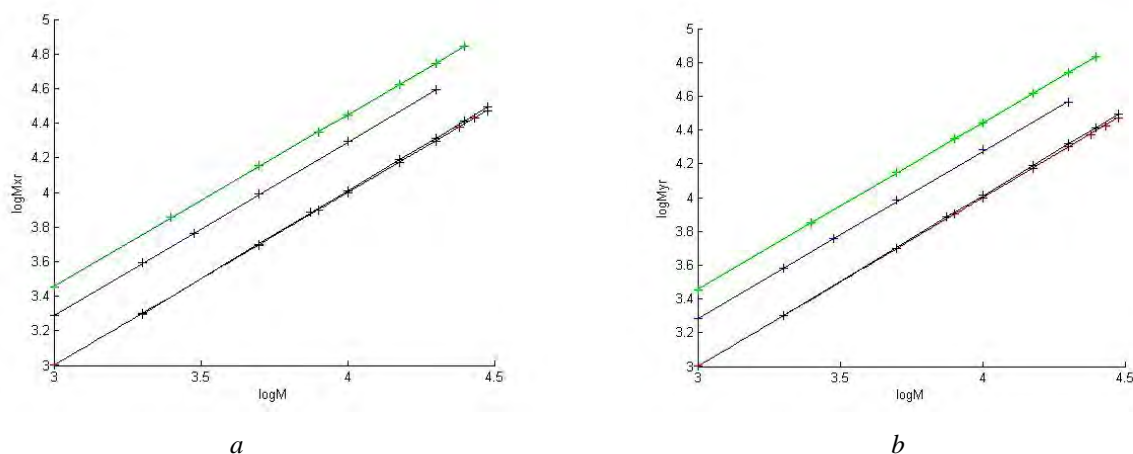


Fig. 1. The graphs of the relations $\log M \rightarrow \log M_{xr}$ (a) and $\log M \rightarrow \log M_{yr}$ (b) for JCM-5000 (red), JSM 7100F (black), DSM-960 A (blue), SEM 106 I (green)

where $s_i = |Ax_i + By_i + C|$ is the distance between the i -th point and the straight line. If $A^2 + B^2 = 1$, then s_i – measures the perpendicular distance between point and line.

The task of minimizing the sum of the squared perpendicular distances between a set of points and a straight line is:

$$\min \sum_{i=1}^N (Ax_i + By_i + C)^2, \quad (6)$$

with the constraint

$$A^2 + B^2 = 1. \quad (7)$$

This problem can be rewritten in the form of a Lagrangian:

$$\min \sum_{i=1}^N (Ax_i + By_i + C)^2 - I(1 - A^2 - B^2), \quad (8)$$

where I is the Lagrange multiplier associated with equation (7). The solution of the normal equations for (8) gives

$$A = \frac{q - (q^2 + 4t^2)^{1/2}}{2t} B \quad \text{and} \quad C = -A\bar{x} - B\bar{y},$$

$$\text{where } q = \left(\sum_{i=1}^N x_i'^2 - \sum_{i=1}^N y_i'^2 \right) \text{ and } t = \sum_{i=1}^N x_i' y_i', \quad (9)$$

(x_i', y_i') – are the translated points centered on the bivariate mean (\bar{x}, \bar{y}) .

From this we find the parameters of equation (1)

$$A_f = 10^C, \quad D_f = 2 - A_f \quad (10)$$

for scales M_{xr} (M_{yr}) in x - and y - direction.

According to the above algorithm, the coefficients A_f and the values of D_f for fractal scales along the x and y axes were calculated using MatLab [Gonzalez, Woods, Eddins, 2006] (see Table 2). Calculations are performed using measured values of real scales for 4 types of SEM. Note that the images of the test grid at different magnifications obtained on the same SEM have the

same coefficient A_f as the dimension D_f in the specified increase range. Figure 2 shows the result of comparing real and approximated fractal scales with an integer scale for four types of SEM.

The graphs in Fig. 2. show the differences between the integer and the real scales and the integer and the fractal ones in the indicated magnification ranges (see Table 2).

For SEM JCM-5000:

- in x – direction from -0.4% to $+1.4\%$;
- in y – direction from -1.5% to $+2\%$;

For SEM JCM-7100F:

- in x – direction from -4% to $+0.6\%$;
- in y – direction from -4% to -0.4% ;

For SEM DSM-960A:

- in x – direction from -97.5% to -94.5% ;
- in y – direction from -94% to -84% ;

For SEM 106I:

- in x – direction from -187% to -179% ;
- in y – direction from -186% to -174% .

From the foregoing it can be seen that the real and fractal scales for the JCM-5000 and JSM 7100F do not significantly differ from the integer scales. For DSM-960A and SEM 106I, significant deviations from integer scales are obtained for both the real and the fractal scales. The performed calculations gave the refined values of the proportionality coefficients A_{xf} (A_{yf}) for the DSM-960A and the SEM 106I (see Table 2).

Therefore, without taking into account the scale factors found, the measurement results for the DSM-960A and SEM 106I are not correct and will lead to significant errors in determining the quantitative characteristics in the study of micro surfaces. The results of studies of these SEMs and real scales of digital SEM images were obtained earlier in [Ivanchuk, Barfels, Heeg, Heger, 2013; Ivanchuk, 2013, 2014; Ivanchuk, Chekajlo, 2014].

Table 2

The values of the coefficients A_{xf} (A_{yf}) and the exponential factors D_{xf} (D_{yf}) of fractal scales M_{xr} (M_{yr})

| № | SEM | Range M^x | A_{xf} | D_{xf} | A_{yf} | D_{yf} |
|---|--------------------------------------|---------------------------------------|------------|------------|------------|------------|
| 1 | JCM-5000 (NeoScope) (JEOL, Japan) | 1000 ^x -30000 ^x | 1.02868436 | 1.00399655 | 1.05475106 | 1.00625075 |
| 2 | JSM 7100F (JEOL, Japan) | 2000 ^x -30000 ^x | 0.86324953 | 0.98177745 | 0.89896265 | 0.98569637 |
| 3 | DSM-960A (Zeiss) | 1000 ^x -20000 ^x | 1.92949231 | 0.99933573 | 2.08935202 | 1.01200954 |
| 4 | SEM 106I (Ukraine) | 1000 ^x -25000 ^x | 3.04724281 | 1.00869793 | 3.10717019 | 1.01240569 |

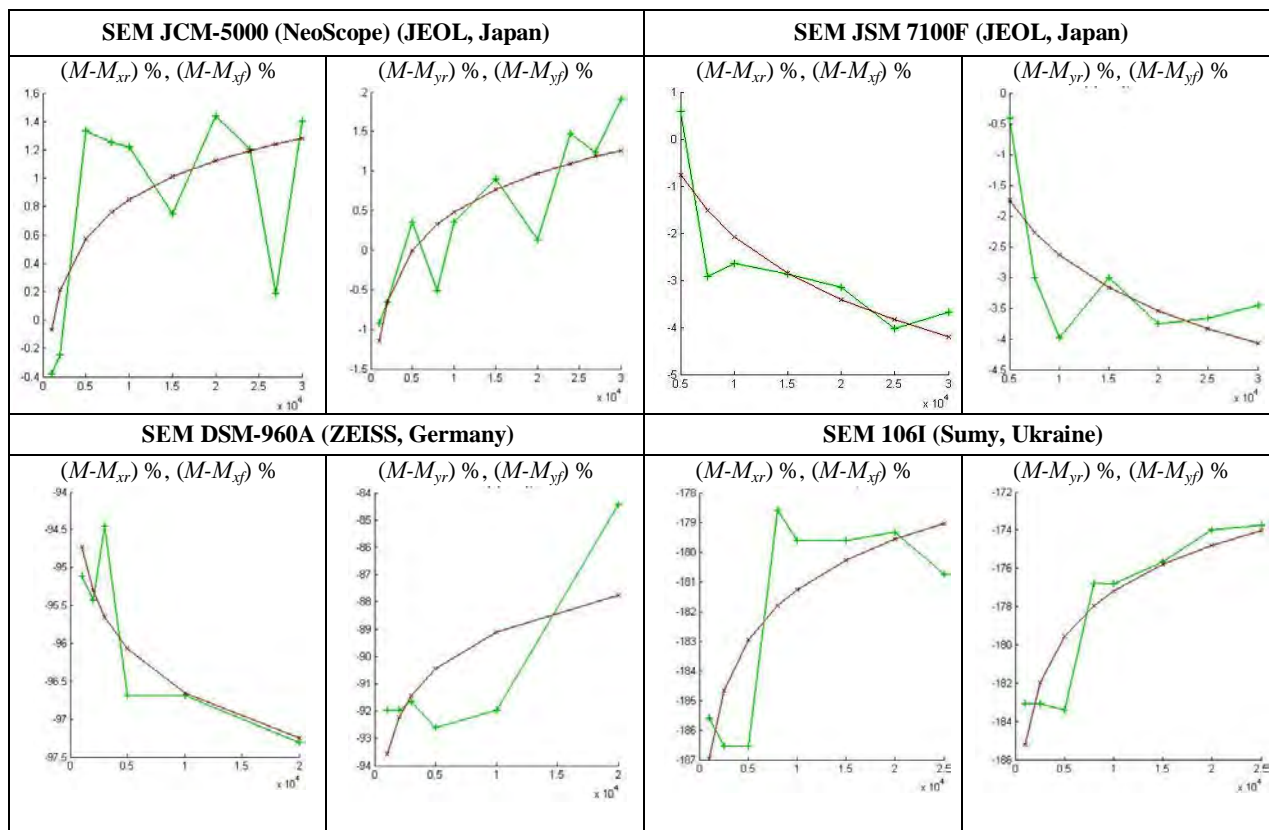


Fig. 2. The relationship between the differences $(M-M_r) \%$ (green), $(M-M_f) \%$ (red) and the integer scales M in x - and y -direction. M_r is the real scale, M_f is the fractal scale

It is known that the fractal dimension is theoretically between one and two for the one-dimensional objects. Note that for JSM 7100F and DSM-960A the experimental values of exponential factor are less than one. Then, the value of A_f will be interpreted as the similarity coefficient, and the exponential factor D_f as the *scaling factor* [Potapov, Gulyaev, Nikitov, Pakhomov, Herman, 2008]. Below are the results of the practical application of fractal scales (hereinafter we leave the term “fractal scale”).

Calculation of the range of increase in the test grid using fractal scales

We define the minimum scale M_0 of the test grid so that the grid test spacing in the SEM image is equal to the pixel size:

$$M_0 = \frac{p}{r}, \quad (p \geq r), \quad (11)$$

where p is the pixel value of the SEM image in mm , r is the size of the true test grid spacing in mm (for the test grid $r = 1/1425 mm$).

It follows that the test grid spacing Δh in pixels on the M -scale image is

$$\Delta h = M \cdot \frac{r}{p}. \quad (12)$$

Then the number of nodes of the test grid on the M -scale image of the size $(W \times H)$ in pixels is in the horizontal direction:

$$n_x = [W / \Delta x] + 1, \quad (13)$$

in the vertical direction:

$$n_y = [H / \Delta y] + 1, \quad (14)$$

where Δx (Δy) the test grid spacing on the M -scale image in the horizontal (vertical) direction, defined by (12). The values in brackets denote the largest integer that does not exceed the magnitude of the mathematical quotient. The vertical size H of the image is determined without taking into account the information strip (see the photos in Table 3).

We set the maximum magnification of the test grid image to calculate the distortion using a quadratic polynomial of two variables. In this case, the required minimum number of the test grid nodes in the frame is 6. Given that the vertical size

of the image H is less than the horizontal W , it suffices to set the number of nodes in the y direction. So that the nodes are not located on the edges of the image, let's take, for example, $n_y = 4$. The maximum scale is

$$M_{\max} = \Delta y \cdot \frac{r}{p}, \quad (15)$$

where $\Delta y = \frac{H}{n_y - 1}$ is the test grid spacing in pixels. A

pair of values (M_0, M_{\max}) defines the magnification range for SEM images of the test grid.

We determine the resolution R (lin/mm) of the true test grid for the upper boundary of the range of the SEM image increase (see Table 1), necessary for taking into account the distortion using a quadratic polynomial of two variables. The maximum resolution is

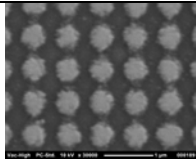
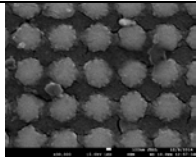

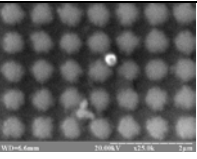
$$R = \frac{M_{\max} \cdot (n_y - 1)}{H \cdot p} \quad (16)$$

where M_{\max} is the maximum scale specified in the technical characteristics of the SEM, n_y, H, p have the same values as in the previous formulas.

Table 3 shows the specifications of SEM images of the test grid, calculated for 4 types of SEM. The size of the test grid (the number of nodes horizontally and vertically) on the SEM images is determined using the maximum values of the scales M, M_r, M_f [Ivanchuk, 2015; Ivanchuk, Tumska, 2015, 2017; Kostyshyn, Mustafin, 1982]. For JCM-5000 and JSM 7100F, the calculated number of nodes for the three types of scales are the same, and the sizes of the test grids differ by not more than one row (column) from their sizes in the photos in Table 3. The discrepancy in the number of rows (columns) is explained by the inclusion of nodes cut by the horizontal (vertical) sides of the frame. For DSM 960A and SEM 106I, grid sizes computed using integer scales are incorrect, whereas for real and fractal scales, the results are similar to the previous SEMs. Since for SEM 106I all nodes of the test grid are completely in the frame and the calculation results give the exact number of nodes in the image.

Table 3

The specifications of digital images of the test grid for different SEMs

| SEM | JCM-5000 (NeoScope) | JSM 7100F | DSM-960A | SEM 106 I |
|---|---|---|--|---|
| Image of the test grid |  |  |  |  |
| Scale M | 30000 ^x | 30000 ^x | 20000 ^x | 25000 ^x |
| Real scale M_{xr} | 29578.86 ^x | 31104.11 ^x | 39462.60 ^x | 70190.65 ^x |
| Real scale M_{yr} | 29426.72 ^x | 31037.31 ^x | 36886.22 ^x | 68431.17 ^x |
| Fractal scale M_{xf} | 29614.91 ^x | 31249.43 ^x | 38844.55 ^x | 69758.01 ^x |
| Fractal scale M_{yf} | 29667.84 ^x | 31253.74 ^x | 37101.22 ^x | 68508.67 ^x |
| The size $n_x \times n_y$ of the test grid in the image in scales M, M_r, M_f | 6×5 6×5 6×5 | 6×5 6×5 6×5 | 16×12 8×7 8×7 | 20×14 7×5 7×5 |
| Magnification range for the test grid with a resolution 1425 lin/mm | from 130 ^x to 44467 ^x | from 134 ^x to 42927 ^x | from 377 ^x to 75406 ^x | from 377 ^x to 111850 ^x |
| Digital image, pixels | 1280x1080 | 1280x1024 | 800x600 | 1280x960 |
| Pixel size, mm | 0.09132 | 0.09375 | 0.26450 | 0.26450 |
| Test grid resolution (lin/mm) for maximum magnification | 1282 for $M=40000^x$ | 9589 for $M=300000^x$ | 3439 for $M_f=181950^x$ (instead of $M = 100000^x$) | 10156 for $M_f=797150^x$ (instead of $M = 300000^x$) |

The last row of Table 3 gives the resolution of the test grids for the values of the upper range of magnifications specified in the technical specifications in Table 1 (see note to (16)). The resolution of test grids for DSM-960A and SEM 106I are determined from the values of fractal scales calculated from the maximum values of integer scales.

Calculation of distortion values of the image coordinates of the test grid using fractal scales for various types of SEM

The values of the distortions of the coordinates of the images of the test grid along the x and y axes are calculated using a cubic polynomial of two variables. The input data are: resolution of the test grid (lin / mm); list of the increase values the set on the device scale; parameters of fractal scales (A_{xf} , D_{xf}) and (A_{yf} , D_{yf}). For each increase value from the above list, the coordinates of the centers of the nodes of the test grid are measured manually by the operator or are automatically recognized. This means that the node centers are recognized using the developed software, and their coordinates are calculated and written to a file [Ivanchuk, Tumska [Ivanchuk, Tumska, 2017].

The technological scheme of approximating the values of the distortions of the image coordinates of the test grid consist of the following steps:

1. Input the coordinate center of the nodes (solution points and control points) of the test grid image in an integer scale M .
2. Definition of the value of the fractal scale (1).
3. Calculation of the test grid spacing in the magnification scale.
4. Formation of the layout of the location of solution points and control points.
5. Calculation of true coordinate center of the nodes of the test grid in the magnification scale.
6. Definition of the coefficients of the cubic polynomials of two variables in x - and y -directions.
7. Estimation of the accuracy of the results of approximation using the solution points and the control points.
8. Construction of vector diagrams.

The remainder describes the individual steps of the proposed technological scheme using of the scale factor in detail.

First, from the measured (recognized) coordinates (x_{mr} , y_{mr}) (mm), we find the corresponding true coordinates (x_{tr} , y_{tr}) (mm) of the test grid in the magnification scale

$$\begin{aligned} x_{tr}(y_{tr}) &= k_x(k_y) \cdot h_x(h_y), \\ h_x(h_y) &= r \cdot M_x(M_y), \end{aligned} \quad (17)$$

where ($r = 1/1425$ is the true grid spacing in mm); M_x (M_y) – given real or fractal scales calculated by (1). The number of lines (spacings) k_x (k_y) from the origin (central node) to the measured point, respectively, in x - and y -direction is:

$$k_x(k_y) = [x_{mr}(y_{mr}) / h_x(h_y)]. \quad (18)$$

(Square brackets here mean rounding up the results to an integer value.)

Note that the number of lines in the test grid image is inversely proportional to the scale value.

Therefore, if the scale is smaller than the real one, when calculating the number of lines of the test grid using the measured (computed) coordinates of the points, the error accumulates closer to the edges of the image and one or two additional lines appear.

It follows that you need to know as accurately as possible the real increase, and the distance between the nodes of the approximation grid should be increased in order to obtain the exact value of k_x (k_y) by (18). These remarks are most important for scales 1000^x , 2000^x , where small changes in the scale values can lead to a change in the value of k_x (k_y).

Problems arise when determining the values of k_x (k_y) for magnification scales in the range $1000^x - 2000^x$ where the grid spacing is of the same order of value as the measurement accuracy (1-3 pixels). For example, the grid spacing in x -direction in a scale of 1000^x , calculated using a fractal scale (12), is (in pixels): $h_x=7.7$ for JCM-5000, $h_x=7.5$ for JSM 7100F, $h_x=5.1$ for DSM-960A, $h_x=7.6$ for SEM 106I.

As experience shows for a scale of 1000^x , the use of a real (fractal) scale makes it possible to almost accurately determine the number of intervals k_x (k_y) using the measured coordinates and finding the corresponding true coordinates.

Second, to obtain a picture of geometric distortions, the measured points are located

symmetrically with respect to the central node of the test grid. In addition, the measured points are divided into solutions points to determine the coefficients of the polynomial and control points to evaluate the accuracy of the calculation results. When automatic recognition of the centers of nodes is done by software, it is necessary to divide the resulting array of points into a solution and control points.

For this purpose, for each scale, we form (manually or automatically) a layout for placing points for solution and control. Namely, we list the exact number of lines k'_x (k'_y) relative to the central node of the test grid.

For example, for JCM-5000 in a 1000^x scale, the layout of the points for the size test grid (167×134) is:

$$k'_x = [-82 \ -74 \ -66 \ -58 \ -50 \ -42 \ -34 \ -26 \ -18 \ -9 \ 0 \ 9 \ 18 \ 26 \ 34 \ 42 \ 50 \ 58 \ 66 \ 74 \ 82],$$

$$k'_y = [65 \ 57 \ 49 \ 41 \ 33 \ 25 \ 17 \ 9 \ 0 \ -9 \ -17 \ -25 \ -33 \ -41 \ -49 \ -57 \ -65].$$

According to the given list, we form two matrices $[x_{ij}]$ and $[y_{ij}]$ of size (17×21) , where the coordinates of solution and control points are

staggered (see Fig. 3). Also, we use the given list of nodes to correct the values of k_x (k_y), calculated from the measured (recognized) coordinates (18). The value k_x (k_y) is replaced by k'_x (k'_y) from the above list if the number of lines k_x (k_y) is not equal to the number k'_x (k'_y), and $|k_x - k'_x| < d$ ($|k_y - k'_y| < d$), where d is the tolerance value (the specified number of lines). The tolerance value d is selected depending on the value of the increase, the greater the scale, the smaller the tolerance. For example, for 1000^x the tolerance is $d = 3$, to increase more than 2000^x is $d = 0.5$.

For JCM-5000 in an integer scale $M = 1000^x$ for the two extreme rows of the grid, when calculating the values of k_y , we get values that are different from the values given in the list by one line: $k_y = 66$ ($k'_y = 65$), $k_y = 58$ ($k'_y = 57$), $k_y = -58$ ($k'_y = -57$), $k_y = -65$ ($k'_y = -66$). For the same calculations performed using real or fractal scales, there are no additional lines at the edges of the test grid. Since the spacing values h_x (h_y) are larger than for integer scales, the value of k_x (k_y) is determined exactly.

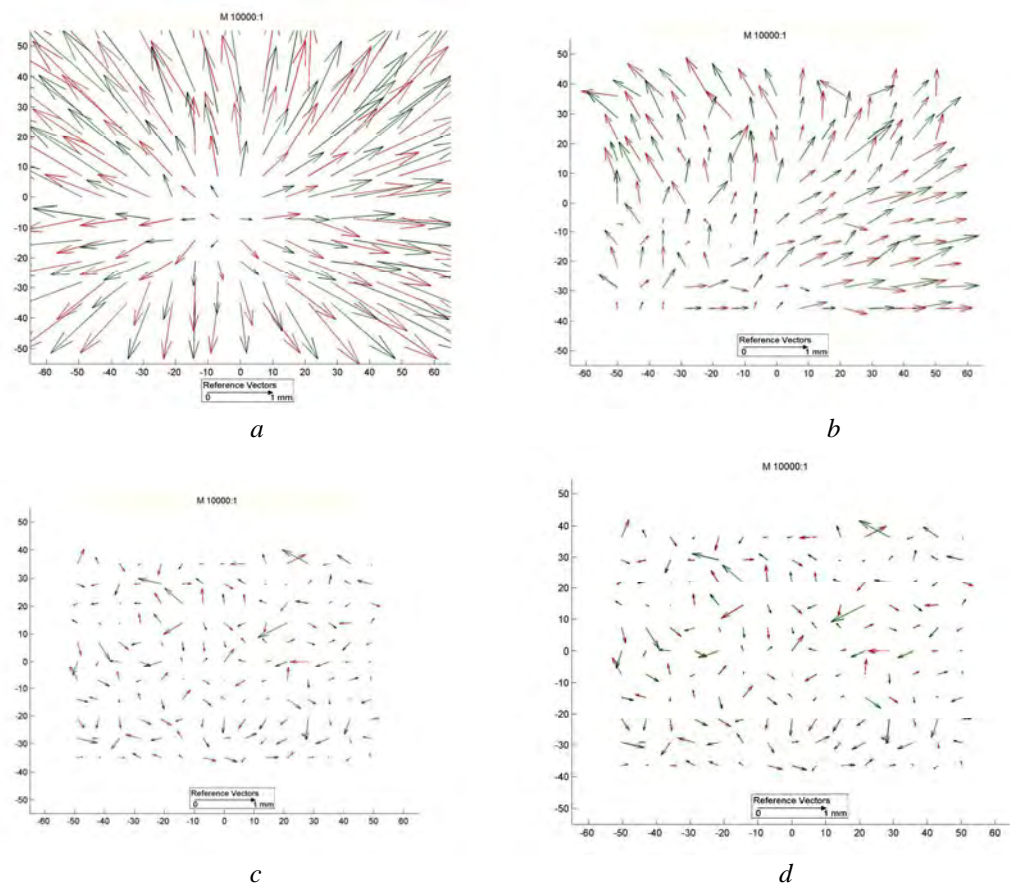


Fig. 3. Vector diagrams of geometric distortions in the SEM image before (a, b) and after the polynomial approximation (c, d). Computation of distortions using an integer scale (a, c), and a fractal scale (b, d)

For example, the spacing of the test grid is (in mm): $h_x = h_y = 0.7018$ for integer scale ($M = 1000^x$); $h_{xr} = 0.7044$, $h_{yr} = 0.7082$ for real scale ($M_{xr} = 1003.80^x$, $M_{yr} = 1009.23^x$); $h_{xf} = 0.7022$, $h_{yf} = 0.7089$ for fractal scale ($M_{xf} = 1000.67^x$, $M_{yf} = 1009.23^x$). If the location of the points for approximation is given, then we can correct the erroneous values of k_x (k_y) using the program.

Third, for an example for JSM 7100F using the integer scale $M = 10000^x$ and the respective fractal scale, the results of the approximation are compared. Figures 3a and b show the vector diagrams of geometric distortions of images determined by the coordinates of the nodes of the test grid, using the integer (a) and the fractal (b) scales. Geometric distortions of the SEM image are defined as the difference between the measured (in mm) and true coordinates (in mm) of the test grid nodes:

$$\Delta x (\Delta y) = x_{mr} (y_{mr}) - x_{tr} (y_{tr}). \quad (19)$$

Vector diagrams show the direction of real displacement of points relative to undistorted (true) positions. Note that Fig. 3a ($M = 10000^x$) illustrates the radial character of the distortions from the center of the SEM image to the edges. In Fig. 3b, using the fractal scales ($M_{xf} = 10207.39^x$, $M_{yf} = 10263.96^x$), we see a picture of the true distortions of the SEM image. The approximation results performed for integer and fractal scales using the cubic polynomial of two variables show the same picture of the residual distortions (Fig. 3, c, d). Vectors length is increased by 20, for clarity. Based on the studies carried out, the following conclusions can be drawn.

Scientific novelty

The technique developed by the authors for obtaining fractal and metric characteristics of SEM images was performed for the first time in Ukraine. The proposed methodology is accompanied at all stages by the author's software and demonstrated its effectiveness and expediency.

The practical significance

The application of this method of establishing and accounting for the fractal and metric characteristics of digital SEM images makes it

possible to more precisely determine the real values of the increases (scales) of digital SEM images and the values of their geometric distortions. Taking into account these characteristics of SEM images makes it possible to significantly improve the accuracy of obtaining spatial quantitative parameters of the micro surfaces of research facilities, and consequently improve their operational and economic characteristics. The obtained characteristics can be additional important quantitative parameters for revealing the features of digital SEM images.

Conclusions

1. An analytical relationship has been established the increase between the set on the device scale and the "fractal" increase (scale). For 4 types of SEM, the similar coefficients A_f and the exponents D_f for the fractal scales along the x and y axes are calculated. It is shown that the images of the test object obtained on the same SEM at different scales have the same fractal scale parameters that can be used as additional quantitative characteristics of SEM.

2. From the analysis of the series of multiscale SEM images it is established that for the JCM-5000 (NeoScope) and JSM 7100F the real and fractal scales are the least different compared to the increases of the set on the device scale. In addition, for these SEM, the anisotropy of the distortions is the least pronounced. It should be noted that for the DSM-960A and SEM 106I, the metric characteristics for the entire range of increases (scales) do not correspond to the magnifications of the set on the scale of the device.

3. Formulas for calculating the possible range of magnifications of the test object images are obtained and given depending on the spacing value of the test object, pixel size, and scale. For 4 types of SEM, the results of calculating the magnification ranges are given. The maximum magnification was determined taking into account the possibility of determining distortions with respect to a quadratic polynomial of two variables.

4. The resolutions of the test objects that are suitable for determining the values of the distortions of the images of the test object at the maximum magnifications specified in the technical specifications of the SEM are calculated.

5. Features of the algorithm for calculating distortion values for automatic recognition of the centers of nodes in the image of a test object are given. It is shown that for small magnifications ($1000^x - 2000^x$) the presence of a layout of placement of solution points and control points with an optimal interval avoids errors in finding the true coordinates of test grid nodes corresponding to the recognized (measured) points.

6. Vector diagrams constructed using the fractal values of increases show a picture of real distortions. Using the magnifications (scales) the set on the device scale allows display of basically only radial distortions in the form of vectors from the center of the image to the edges. After approximation by a cubic polynomial of two variables, the residual distortions are significantly (2–10 times) less than the real ones and are 1–2 pixels, no matter what type of magnification (scale) of SEM images was used.

7. The obtained relationships for establishing the values of fractal scales allow automatic determination of the actual increase (scale) of the SEM images and, together with the calculated coefficients of the polynomials, effectively eliminate their distortions. This significantly improves the accuracy of obtaining spatial coordinates of the points of the micro surfaces of the research objects and the creation of their digital terrain models.

REFERENCES

- Anisichenko V. S., Vadivasova T. E. *Lektsii po nelineynoy dinamike: Uchebnoye posobiye dlya studentov vuzov. obuchayushchikhsya po spetsialnosti "Radiofizika i elektronika" i "Fizika"* [Lectures on nonlinear dynamics: A manual for university students studying in the specialty: "Radiophysics and Electronics" and "Physics"], Saratov: Saratov University Press, 2010, 322 p.
- Bobro Yu. G., Melnik V.N., Voloshin V.U., Shostak A. V. *Printsipy fraktalnosti v mekhanike razrusheniya metallov* [Principles of fractality in the mechanics of the destruction of metals], Proceedings of the Russian Academy of Sciences. Metals, 1997, No. 2, pp. 119–122.
- Bovik A.I. *Handbook of Image and Video Processing*. Academic Press., A Harcourt Science and Technology Company, 2000, 891 p.
- Boyde A., Ross H. F. *Photogrammetry and Scanning electron microscopy*. Photogrammetric Record. 1975, vol. 8, no. 46, pp. 408–457.
- Burkhardt R. *Untersuchungen zur kalibrirung eines Elektronen mikroskopes*. Mitt. geod. Inst. Techn. Univ. Graz. 1980, no. 35.
- Feder E. *Fraktaly: Per. s angl.* [Fractals: Translation from English], Moscow, MIR, 1991, 254 p.
- Ghosh S. K. *Photogrammetric calibration of a scanning electron microscope*. *Photogrammetria*. 1975, vol. 31, no. 31, pp. 91–114.
- Ghosh S. K., Nagaraja H. *Scanning Electron Micrography and Photogrammetry*. *Photogrammetric Engineering and Remote Sensing*. 1976, vol. 42, no. 5. pp. 649–657.
- Gonzalez R. Ñ., Woods R. E., Eddins S. L. *Cyfrovaja obrabotka izobrazhenij v srede MATLAB* [Digital Image Processing using MATLAB]. Moscow, *Technosfera*, 2006. 616 p.
- Cromley R. G. *Digital Cartography*. 1992 by Prentice-Hall. 317 p.
- Howell P. *A practical method for the correction of distortions in SEM photogrammetry*. Proc. Of the Annual Scanning Electron Microscope Symposium. Chicago, Illinois. 1975, pp. 199–206.
- Ivanchuk O. M., Khrupin I. V. *Struktura ta funkcii prohramnoho kompleksu "Dimicros" dlja opracjuvannja REM-zobrazhen na cufrovij fotohrammetrychnij stanciji* [Structure and function of the program complex "Dimicros" processing of SEM images on a digital photogrammetric station], *Recent advances in geodetic science and industry*, Lviv, 2012, issue 1(23), pp. 193–197.
- Ivanchuk O. M. *Doslidzhennja tochnosti vyznachennja dijsnych velychyn zbilshennja (masshtabu) cyfrovych REM-zobrazhen, otrymanykh na REM JCM-5000 (NeoScope) firmy JEOL* [Investigation of the accuracy of the actual values increase (scale) digital SEM images obtained by SEM JCM-5000 (NeoScope) company JEOL], *Geodesy, cartography and aerial photography*, Lviv, 2012, issue 76, pp. 80–84.
- Ivanchuk O. M., Barfels T., Heeg J., Heger W. *Doslidzhennja velychyn heometrychnykh spotvoren cyfrovych REM-zobrazhen, otrymanykh na REM DSM-960A (Carl Zeiss, Nimechchyna) ta tochnosti jich vrachuvannja* [Research quantities of geometric distortion of digital SEM images obtained by SEM DSM-960A (Carl Zeiss, Germany) and the accuracy of their incorporation], *Geodesy, cartography and aerial photography*, Lviv, 2013, issue 78, pp. 120–126.
- Ivanchuk O. *Doslidzhennja heometrychnykh spotvoren cyfrovych REM-zobrazhen, otrymanykh na REM JCM-5000 (NeoScope) ta jikh aproksymacija* [Researching geometric distortion digital SEM images obtained on SEM JCM-5000 (NeoScope)]

- and their approximation], Scientific Papers of Donetsk National Technical University. Series: geological. Donetsk, 2013. Vol. 1 (18), pp. 91–97.
- Ivanchuk O., Chekajlo M. *Doslidzhennja pokhybok zbilshennja (masshtabu) cyfrovykh REM-zobrazhen, otrymanykh na REM-106I (Sumy, Ukraina) za dopomohuju specialnykh test-objektiv* [Research errors increase (scale) digital SEM images obtained on SEM-106I (Sumy, Ukraine) with special test facilities], *Geodesy, cartography and aerial photography*, Lviv, 2014, issue 79, pp. 82–88.
- Ivanchuk O. *Doslidzhennja heometrychnykh spotvoren cyfrovykh REM-zobrazhen, otrymanykh na REM-106I (Sumy, Ukraina)* [Researching geometric distortion digital SEM images obtained at the SEM-106 and (Sumy, Ukraine)], *Recent advances in geodetic science and industry*, Lviv, 2014, issue II (28), pp. 74–77.
- Ivanchuk O. *Osoblyvosti kalibruvannja heometrychnykh spotvoren cyfrovykh REM-zobrazhen, otrymanykh na riznykh REM* [Features Calibration geometric distortion of digital SEM images obtained at different SEM], *Recent advances in geodetic science and industry*, Lviv, 2015, issue I (29), pp. 68–173.
- Ivanchuk O. *Doslidzhennja heometrychnykh spotvoren cyfrovykh REM-zobrazhen, otrymanykh na REM JSM-7100F (JEOL, Japonija) ta tochnist jikh aproksymaciji* [Research geometric distortion of SEM digital images obtained with SEM JSM-7100F (JEOL, Japan) and the accuracy of approximation], *Geodesy, cartography and aerial photography*, Lviv, 2015, issue 81, pp. 101–109.
- Ivanchuk O., Tumska O. Development and research of technology for automation of the calibration and account of digital SEM images having geometric distortion obtained with JCM –5000 (Neoscope) (JEOL, Japan), *Geodesy, cartography and aerial photography*, Lviv, 2016, issue 84, pp. 56–64.
- Ivanchuk O., Tumska O. *Metodyka avtomatyzovanogo vyznachennja koordynat tsestriv vuzliv test-objekta za yogo REM-zobrazhennyamy z vykorystannjam zasobiv MatLab* [Technique of automated determination of the coordinates of the test-object nodes by its SEM images using MatLab tools], *Recent advances in geodetic science and industry*, Lviv, 2017, issue I (33), pp. 158–165.
- Ivanchuk O., Tumska O. *Porivnyalnyy analiz statystychnykh ta skeylingovykh kharakterystyk REM-zobrazhen test-objekta, otrymanykh na riznykh typakh REM* [Comparative analysis of the statistical and scaling characteristics of SEM images, obtained with different types of SEM], *Recent advances in geodetic science and industry*, Lviv, 2017, issue II (34), pp. 119–131.
- Kostyshyn M.T., Mustafin K.S. *Kvantovaja elektronika* [Quantum Electronics], Kyiv, 1982, issue 23, pp. 29–33.
- Kalantarov E. I., Sagyndykova M. Zh. *Photogrammetricheskaja kalibrovka elektronnykh mikroskopov* [Photogrammetric calibration of electron microscopes], *Proceedings of the universities. Surveying and aerial photography*, Moscow, 1983, issue 4, pp. 76–80.
- Mandelbrot B. *The fractal geometry of nature*. N. Y.: Freeman, 1983, 469 p.
- Melnik V. N., Sokolov V. N., Ivanchuk O. M., Tumska O. V., Shebatinov M. P. *Kalibrovka geometricheskikh iskazhenij REM-snimkov* [Calibration of geometric distortion SEM images], Manuscript deposited at VINITI, Moscow, 1984, issue 528, 18 p.
- Melnik V. N., Sokolov V. N. *Fraktalnaya i stereometricheskaya otsenki REM-izobrazhenij sherokhovatykh poverkhnostey* [Fractal and stereometric estimations of SEM images of rough surfaces], *Proceedings of the Russian Academy of Sciences. The series is physical*, 1993, no. 8, pp. 99–105.
- Melnik V. N., Bobro Yu. G., Shostak A. V., Voloshin V. U. *Opredeleniye fraktalnosti poverkhnostey razrusheniya po dannym REM-stereoizmerenij* [Determination of the fractality of fracture surfaces according to SEM-stereo measurements], *Friction and wear*, 1996, T. 16, no. 6, pp. 38–41.
- Melnik V. M., Voloshin V. U., Tarasyuk F. P., J. Blinder Yu.S. *Metody kilkisnoj kharakterystyky mikrostruktury gruntu* [Methods of quantitative characterization of soil microstructure], *Bulletin of Lviv State University. Geographic series*, Ivan Franko National University of Lviv; Editor-in-Chief S. Poznyak, Lviv, 1999, no. 25, pp. 24–27.
- Melnik V. M., Voloshin V. U. *Otsinka destruktivnykh zmin kistkovoji tkanyny metodamy strukturnoji funktsiji ta fraktalnogo analizu* [Evaluation of destructive changes in bone tissue by the methods of structural function and fractal analysis], *Scientific Bulletin of the Volyn State University named after Lesya Ukrainka*, Lutsk, 2002, no. 3, pp. 166–171.
- Melnik V. M., Shostak A. V. *Rastrovo-elektronna stereomikrofraktohrafiya* [Raster electron stereomicrofractography], Luck, Vezha, 2009, 469 p.
- Potapov A. A., Gulyaev Yu. V., Nikitov S. A., Pakhomov A. A., Herman V. A. *Noveyshiye metody obrabotki izobrazhenij* [The newest methods of image processing], Moscow, *FIZMATLIT*, 2008, 496 p.
- Richardson L. *The Problem of Contiguity: An Appendix of Statistic of Deadly Quarrels*. *General Systems Year Book*. 1961, no. 6, pp. 139–187.
- Shostak A. V. *Metody i modeli mikrofraktohrafiyi u prukladnykh naukovykh doslidzhennjach*. *Dokt. Diss.* [Methods and models of microfractography in applied research. Doct. Diss.]. Kyiv, 2012. 28 p.

О. ІВАНЧУК^{1*}, О. ТУМСЬКА²

¹ Кафедра фотограмметрії та геоінформатики, Національний університет “Львівська політехніка”, вул. С. Бандери, 12, Львів, Україна, 79013, тел. +38(068)0720575, ел. пошта: ivanchuk_oleh@ukr.net

² Кафедра фотограмметрії та геоінформатики, Національний університет “Львівська політехніка”, вул. С. Бандери, 12, Львів, Україна, 79013, тел. +38(050)7455711, ел. пошта: ol.tums@gmail.com

ДОСЛІДЖЕННЯ ФРАКТАЛЬНИХ ТА МЕТРИЧНИХ ВЛАСТИВОСТЕЙ ЗОБРАЖЕНЬ ЗА ДАНИМИ ВИМІРЮВАНЬ РІЗНОМАСШТАБНИХ ЦИФРОВИХ РЕМ-ЗОБРАЖЕНЬ ТЕСТ-ОБ’ЄКТА

Мета. Метою цієї роботи є встановлення та дослідження фрактальних та метричних характеристик зображень, отриманих за допомогою растрових електронних мікроскопів (РЕМ). **Методика.** Дослідження ґрунтуються на опрацюванні даних вимірювань цифрових РЕМ-зображень тест-об’єкта, отриманих на чотирьох типах сучасних РЕМ у діапазоні збільшень від 1000^x до 30000^x (крат). **Результати.** Встановлено аналітичне співвідношення між фіксованим на шкалі приладу і “фрактальним” збільшенням (масштабом). Виконано розрахунок коефіцієнтів подібності A_f та експоненціальних показників D_f для фрактальних збільшень (масштабів) уздовж осей x та y для 4-х типів РЕМ. Отримано і наведено формули для розрахунку можливого діапазону збільшень зображень тест-об’єкта залежно від кроку тест-об’єкта, розміру пікселя та масштабу. Отримані співвідношення для обчислення фрактальних масштабів дають змогу автоматично визначити дійсне збільшення (масштаб) РЕМ-зображень і разом з визначеними коефіцієнтами поліномів ефективно усувають їхні дисторсійні спотворення. **Наукова новизна.** Розроблена авторами методика отримання фрактальних та метричних характеристик РЕМ-зображень виконана вперше в Україні. Запропонована методика супроводжується на всіх її етапах авторським програмним забезпеченням і показала свою ефективність та доцільність. **Практична значущість.** Застосування цієї методики встановлення та врахування фрактальних і метричних характеристик цифрових РЕМ-зображень дає змогу з більшою точністю визначати дійсні значення збільшень (масштабів) цифрових РЕМ-зображень та величини їхніх геометричних спотворень. Врахування цих характеристик РЕМ-зображень дає змогу суттєво підвищити точність отримання просторових кількісних параметрів мікроповерхонь дослідних об’єктів, а, отже, покращити їхні експлуатаційні та економічні характеристики. Отримані характеристики можуть бути додатковими важливими кількісними параметрами для виявлення особливостей цифрових РЕМ зображень.

Ключові слова: растровий електронний мікроскоп (РЕМ); тест-об’єкт; цифрове РЕМ-зображення; фрактальні та метричні властивості цифрових РЕМ-зображень; дійсні збільшення (масштаби); геометричні спотворення цифрових РЕМ-зображень.

Received 10.05.2017